

MICROWAVE FARADAY EFFECT IN n -TYPE GERMANIUM

by A. BOUWKNEGT*) and J. VOLGER

Fysisch Laboratorium der Rijksuniversiteit, Utrecht, Nederland

Synopsis

The Faraday rotation, ellipticity and the accompanying magneto-absorption were determined from measurements with the crossed wave guide coupler device, at room temperature, at 24.9 GHz. The complex conductivity tensor elements of n -type germanium were deduced from this complete Faraday effect, with the magnetic induction \mathbf{B} parallel to the [001] direction of the crystal. The effective mass could be determined from these experiments. Moreover, the off-diagonal magnetoconductivity was examined. The polarization anisotropy of the Faraday effect was measured with $\mathbf{B} // [011]$. Results of these measurements on the rotation indicate an almost isotropic relaxation time at room temperature.

1. *Introduction.* Measurements of the microwave Faraday effect in semiconductors have been reported by various authors¹⁻⁴). In the microwave frequency range the collision frequency of the current carriers can already be of the same order of magnitude as the frequency of the electric field. Thus, interesting relaxation effects may be observed in the microwave range. In general the relations between the Faraday effect and the quantities of interest, which are the relaxation time and the effective mass, are rather complicated, and the relaxation effects are present in the Faraday effect rather implicitly.

It is the first purpose of the present paper to point out the possibility of determining the complex conductivity tensor elements from measurements of the complete Faraday effect, i.e. of the rotation, ellipticity and the phase and amplitude of the major axis of the ellipse, described by the microwave electric field vector. In these tensor elements the relaxation effects can be studied fairly directly.

The second purpose of this paper is to report on the potential possibilities of a study of the polarization anisotropy of the Faraday effect. This anisotropy occurs if one rotates the direction of the polarization of the incident wave with respect to the crystal axes, for a fixed orientation of the magnetic field.

*) Present address: Philips Research Laboratories, Eindhoven, Nederland.

2. *Theory of the Faraday effect.* The theory of the Faraday effect will be given briefly. Partly it follows closely the treatment given by Donovan and Webster^{5) 6)}.

Let us consider plane waves, written as $\exp(-i\omega t + i\gamma z)$, where ω is the angular frequency, t the time, γ the complex propagation constant and z the coordinate along the direction of propagation. From Maxwell's equations it follows that:

$$\partial^2 \mathbf{E} / \partial z^2 = -\omega^2 \mu_0 \mathbf{D} - i\omega \mu_0 \mathbf{J}, \quad (1)$$

where \mathbf{E} is the electric field, μ_0 the magnetic permeability, \mathbf{D} the electric displacement and \mathbf{J} the current density. If we relate \mathbf{D} and \mathbf{J} with \mathbf{E} through the tensors ε and σ we can write the x and y components of (1) as:

$$\begin{aligned} \partial^2 E_x / \partial z^2 &= \mathfrak{A} E_x + \mathfrak{B} E_y & \text{with: } \mathfrak{A} &= -\omega \mu_0 (\omega \varepsilon_{xx} + i \sigma_{xx}) \\ \partial^2 E_y / \partial z^2 &= \mathfrak{C} E_x + \mathfrak{D} E_y & \mathfrak{B} &= -\omega \mu_0 (\omega \varepsilon_{xy} + i \sigma_{xy}) \end{aligned} \quad (2)$$

and similar expressions for \mathfrak{C} and \mathfrak{D} . ε_{xx} , σ_{xx} etc. are the elements of the ε and σ tensors. A solution of (2) is:

$$\begin{aligned} E_x &= a_1 \exp(i\gamma_+ z) + a_2 \exp(i\gamma_- z) \\ E_y &= b_1 \exp(i\gamma_+ z) + b_2 \exp(i\gamma_- z) \end{aligned} \quad (3)$$

In these and the following formulae the factor $\exp(-i\omega t)$ is omitted for convenience. Combination of equations (2) and (3) yields for γ_{\pm} the expressions:

$$2\gamma_{\pm}^2 = -(\mathfrak{A} + \mathfrak{D}) \pm [(\mathfrak{A} - \mathfrak{D})^2 + 4\mathfrak{B}\mathfrak{C}]^{\frac{1}{2}}. \quad (4)$$

To avoid ambiguities the argument φ of the square root in (4) will be chosen $0 \leq \varphi < \pi$. The choice of the sign in (4) is completely arbitrary at this moment. The coefficients a_1 , a_2 , b_1 and b_2 can be determined by applying the boundary conditions at $z = 0$:

$$E_x = E_0 = a_1 + a_2 \quad E_y = 0 = b_1 + b_2 \quad (5)$$

Combined with equations (2)–(4) this yields:

$$\begin{aligned} a_1 &= \frac{1}{2} E_0 \left[1 - \frac{\mathfrak{A} - \mathfrak{D}}{F} \right] & a_2 &= \frac{1}{2} E_0 \left[1 + \frac{\mathfrak{A} - \mathfrak{D}}{F} \right] \\ b_1 = -b_2 &= E_0 \frac{-\mathfrak{C}}{F} & F &= [(\mathfrak{A} - \mathfrak{D})^2 + 4\mathfrak{B}\mathfrak{C}]^{\frac{1}{2}}. \end{aligned} \quad (6)$$

Consequently, the x and y components of the electric field, as given in (3), are completely determined. In principle the Faraday rotation, ellipticity, and the phase and amplitude of the major axis of the ellipse, which is described by the electric field vector, can be deduced from these field components.

If we interchange the signs preceding the square root in (4) we find that

a_1 and a_2 , and b_1 and b_2 are interchanged too. So, the rotation and ellipticity of the radiation do not depend on any particular sign choice in (4).

In the isotropic case $\epsilon_{xx} = \epsilon_{yy}$, $\epsilon_{xy} = \epsilon_{yx} = 0$, $\sigma_{xx} = \sigma_{yy}$, $\sigma_{xy} = -\sigma_{yx}$. Consequently $i\mathfrak{B} = \omega\mu_0\sigma_{xy}$. For electrons both the real and imaginary parts of σ_{xy} are negative in a positive magnetic field. So, with the adopted sign convention for the square root, we have:

$$\frac{1}{2}[(\mathfrak{A} - \mathfrak{D})^2 + 4\mathfrak{B}\mathfrak{C}]^{\frac{1}{2}} = -i\mathfrak{B}. \quad (7)$$

By combining (7), (6) and (3) we find that the wave with the propagation constant γ_+ , thus with the plus label, is a (circularly polarized) wave rotating clockwise to an observer looking along the $+z$ direction. In the following we shall call such a wave a positive wave. If σ_{xy} changes sign, by reversal of the sign of either the magnetic field or the charge of the carriers, and we use equation (4), the positive wave would be labelled by the subscript $-$. However, the attachment of the label does not influence the substance and the result of the calculation (3)–(6).

In the isotropic case the propagation constants for the positive and negative waves may be written as;

$$\gamma_{\pm}^2 = -\mathfrak{A} \mp i\mathfrak{B} = \omega^2\mu_0\epsilon_l + i\omega\mu_0(\sigma_{xx} \pm i\sigma_{xy}) \quad (8)$$

where ϵ_l is the dielectric constant of the host crystal. In equation (8) the $+$ label always denotes a positive wave. With $\gamma_{\pm} = \alpha_{\pm} + i\beta_{\pm}$ the relations between the properties of the ellipse, described by the electric field vector, and the propagation constants are:

$$-\theta = \frac{1}{2}(\alpha_+ - \alpha_-) z \quad \Delta' = -\tanh \frac{1}{2}(\beta_+ - \beta_-) z = \tanh \Delta \quad (9)$$

where θ is the rotation of the major axis of the ellipse with respect to the initial polarization direction, and Δ' the ellipticity. The rotation is taken positive if the rotation θ is clockwise to an observer looking along the $+z$ direction, Δ' is positive if the electric field of the elliptically polarized wave rotates clockwise to the same observer. Moreover, we have:

$$\begin{aligned} \psi(B) - \psi(0) &= [\frac{1}{2}(\alpha_+ + \alpha_-) - \alpha_0] z \\ E(B)/E(0) &= \exp[-\{\frac{1}{2}(\beta_+ + \beta_-) - \beta_0\} z] \cdot \cosh \frac{1}{2}(\beta_+ - \beta_-) z \end{aligned} \quad (10)$$

where $\psi(B)$ and $E(B)$ denote the phase and amplitude of the major axis of the ellipse.

The quantities θ and Δ' may be considered as the high frequency version of the Hall effect, the quantities appearing in (10) as the high frequency manifestations of the magnetoconductivity. Thus, by measuring the radiating elliptically polarized wave, we may find the quantities:

$$\begin{aligned} \frac{1}{2}(\alpha_+ - \alpha_-) &= -\theta/l & \frac{1}{2}(\alpha_+ + \alpha_-) &= \bar{\alpha} \\ \frac{1}{2}(\beta_+ - \beta_-) &= -\Delta/l & \frac{1}{2}(\beta_+ + \beta_-) &= \bar{\beta} \end{aligned} \quad (11)$$

where θ/l and Δ/l denote the specific rotation and ellipticity.

By splitting equation (8) into real and imaginary parts we find after some rearrangements the relations:

$$\begin{aligned}
 \theta/l \cdot \bar{\alpha} - \Delta/l \cdot \bar{\beta} &= \frac{1}{2} \omega \mu_0 \sigma'_{xy} \\
 \theta/l \cdot \bar{\beta} + \Delta/l \cdot \bar{\alpha} &= \frac{1}{2} \omega \mu_0 \sigma''_{xy} \\
 \bar{\alpha} \cdot \bar{\beta} + \theta/l \cdot \Delta/l &= \frac{1}{2} \omega \mu_0 \sigma'_{xx} \\
 (\theta/l)^2 - (\Delta/l)^2 + \bar{\alpha}^2 - \bar{\beta}^2 &= \omega \mu_0 (\omega \epsilon_l - \sigma''_{xx})
 \end{aligned} \tag{12}$$

So, both the real and imaginary parts of the conductivity tensor elements can be found from a determination of the complete Faraday effect. The relations (12) are very useful for the study of relaxation effects in semiconductors. These effects are manifest in the imaginary parts of the conductivity tensor elements in a fairly direct way. In the Faraday rotation etc. they are present far more implicitly. Relations similar to (12) have been given in a more approximate form by Champlin⁷).

In the anisotropic case ($\sigma_{xx} \neq \sigma_{yy}$ and/or $\sigma_{xy} \neq -\sigma_{yx}$) the matter is more complicated. Then the incident wave is decomposed into two elliptically polarized waves, instead of into two circularly polarized waves, with different propagation constants γ_{\pm} given by equation (4). We assume the conductivity tensor to be:

$$\begin{bmatrix} \sigma_{xx} & \sigma_{xy} \\ -\sigma_{xy} & \sigma_{yy} \end{bmatrix} \tag{13}$$

on coordinates with z along the direction of the magnetic field and x along the direction of polarization of the incident linearly polarized wave (compare equation (5)). The Faraday effect for a wave incident with a polarization direction rotated over an angle φ should be described with a tensor on x', y' coordinates rotated around the z direction over the same angle φ . This tensor is given by:

$$\begin{bmatrix} \sigma_{xx} \cos^2 \varphi + \sigma_{yy} \sin^2 \varphi & \sigma_{xy} + (\sigma_{xx} - \sigma_{yy}) \sin \varphi \cos \varphi \\ -\sigma_{xy} + (\sigma_{xx} - \sigma_{yy}) \sin \varphi \cos \varphi & \sigma_{xx} \sin^2 \varphi + \sigma_{yy} \cos^2 \varphi \end{bmatrix} \tag{14}$$

It turns out that a rotation of the polarization direction with respect to the crystal does not change the value of the propagation constants in (4), but changes the decomposition of the incident linearly polarized wave into elliptically polarized waves. This causes an anisotropy of the Faraday effect. We shall call this anisotropy "polarization anisotropy" in the subsequent paragraphs. Donovan and Webster⁵⁾⁶⁾ showed that in the anisotropic case the rotation and ellipticity depend on both $(\alpha_+ - \alpha_-)$ and $(\beta_+ - \beta_-)$, in contradistinction to the isotropic case (compare equation (9)). Moreover, they pointed out that the polarization anisotropy in n -type germanium should be maximal with the magnetic field applied along the [011] direction of a germanium crystal, and that in this orientation the

anisotropy might be of the order of 20% in the microwave frequency range, if medium magnetic fields were applied.

The conductivity tensor of *n*-type germanium has been calculated by various authors, for example recently by Donovan and Webster⁶⁾ and Krag and Brown⁸⁾, starting from the Boltzmann equation. For convenience of the reader we give the expressions for this tensor in the high frequency case, with the magnetic field applied along the [001] and [011] axes of a germanium crystal, and written down in a coordinate system in which the *z*-coordinate is along the direction of **B**.

a) **B** // [001]

$$\begin{aligned}
 \sigma_{xx} &= \sigma_{yy} = \frac{1}{3}ne \langle (\mu_L + 2\mu_T) \cdot \Gamma \rangle \\
 \sigma_{xy} &= -\sigma_{yx} = \frac{1}{3}neB \langle \mu_T(2\mu_L + \mu_T) \cdot \Gamma \rangle \\
 \sigma_{zz} &= \frac{1}{3}ne \langle (\mu_L + 2\mu_T) \cdot \Gamma + 3B^2\mu_L\mu_T^2 \cdot \Gamma \rangle \\
 1/\Gamma &= 1/\Gamma_{1234} = 1 + \frac{1}{3}\mu_T(2\mu_L + \mu_T) B^2 \\
 z // [001] \quad x // [110] \quad y // [110]
 \end{aligned} \tag{15}$$

b) **B** // [011]

$$\begin{aligned}
 \sigma_{xx} &= \frac{1}{3}ne \langle 3\mu_T\Gamma_{13} + (\mu_T + 2\mu_L) \Gamma_{24} \rangle \\
 \sigma_{yy} &= \frac{1}{3}ne \langle (\mu_L + 2\mu_T)(\Gamma_{13} + \Gamma_{24}) \rangle \\
 \sigma_{xy} &= -\sigma_{yx} = \frac{1}{3}neB \langle \mu_T\{(\mu_L + 2\mu_T) \Gamma_{13} + 3\mu_L\Gamma_{24}\} \rangle \\
 \sigma_{zz} &= \frac{1}{3}ne \langle (\mu_T + 2\mu_L) \Gamma_{13} + 3\mu_T\Gamma_{24} + 3B^2\mu_T^2\mu_L(\Gamma_{13} + \Gamma_{24}) \rangle \\
 1/\Gamma_{13} &= 1 + \frac{1}{3}\mu_T(\mu_L + 2\mu_T) B^2 \\
 1/\Gamma_{24} &= 1 + \mu_T\mu_L B^2 \\
 z // [011] \quad x // [0\bar{1}1] \quad y // [100]
 \end{aligned} \tag{16}$$

$$\mu_L = \frac{e\tau_{//}}{m_{//}(1 - i\omega\tau_{//})}, \quad \mu_T = \frac{e\tau_{\perp}}{m_{\perp}(1 - i\omega\tau_{\perp})}$$

In these formulae the subscripts of the Γ denote the numbers given to the different "valleys" in the reduced crystal momentum space, $m_{//, \perp}$ are the effective masses, $\tau_{//, \perp}$ the relaxation times, n the carrier concentration in the crystal, e the electronic charge, and **B** the magnetic induction. The brackets denote an averaging procedure:

$$\langle g \rangle = \frac{4}{3\sqrt{\pi}} \int_0^{\infty} g(x) x^{\frac{1}{2}} e^{-x} dx. \quad x = E_n/kT \tag{17}$$

over the different possible electron energies E_n . The relaxation time will in general depend on the electron energy.

From equations (15) and (16) the conductivity tensor can be deduced in different approximations and for different assumptions concerning the relaxation time. This subject is treated in some more detail elsewhere⁹⁾.

3. *On the experimental arrangement.* The microwave measuring circuit has been discussed earlier^{4) 9)}. With the crossed wave guide coupler device phase and amplitude of the wave transmitted through a semiconductor slab were measured in two perpendicular directions. From these four measurements the four quantities which define the ellipse, described by the microwave electric field vector, could be deduced.

The electromagnetic field inside the wave guide coupler is complicated, but it seems to be reasonable to approximate this field by plane waves. It proved to be possible to determine experimentally the small corrections which are necessary to convert the values of the Faraday effect as found with the wave guide coupler to plane wave values⁹⁾. The corrections can be applied as long as the changes in the propagation constant $\gamma = \alpha + i\beta$, caused by the magnetic field, are small compared to the zero field value.

4. *Experimental results, isotropic case.* Some measurements were made on an *n*-type germanium crystal, with $\mathbf{B} // [001]$, thus for an "isotropic" orientation (compare (15)). The crystal had a d.c. conductivity $\sigma = 24.7 \Omega^{-1}\text{m}^{-1}$, a Hall mobility $\mu_H = 0.41 \text{ m}^2/\text{V}\cdot\text{s}$, the frequency was 24.9 GHz, the temperature 22°C. From measurements for six values of the thickness d of the crystal, with $d > 2\delta$, where δ is the penetration depth of the microwave electric field, the specific values of the Faraday effect could be determined. These values are given in fig. 1. The experimental errors were estimated from the random deviations of the measured points from a linear dependency on d . Moreover, the zero field plane wave values of the propagation constants were determined with a conventional wave guide technique. The values found were $\alpha_0 = 2.28 \text{ mm}^{-1}$ and $\beta_0 = 1.07 \text{ mm}^{-1}$.

The experimental results were compared with theory. With equations (15) the Faraday effect was calculated for two assumptions regarding the relaxation time: a) τ is a constant, so independent of the energy of the electrons, and b) τ depends on energy as $\tau = u(kT/E_n)^{\frac{1}{2}}$. With these assumptions (15) can be worked out⁹⁾, and calculated with the aid of tabulated integrals¹⁰⁾. The numerical values used in the calculations were: $m_{//}/m_0 = 1.58$, $m_{//}/m_{\perp} = 19.3$, $\epsilon_i/\epsilon_0 = 16.3$ ^{11) 12)}, and the measured values of σ and μ_H . The results of the calculations are given in the curves (a) and (b) for the different assumptions regarding τ .

It is seen that in general the agreement between theory and experiment is good. One may note that, except in the case of the rotation, the agreement is better for the assumption of a constant relaxation time. At first sight the measuring technique may be thought responsible for this effect, the microwave electric field inside the crystal being poorly known. However, in the measurements on the Voigt magneto-absorption¹³⁾, which were made with a conventional wave guide technique, a same kind of deviations from the

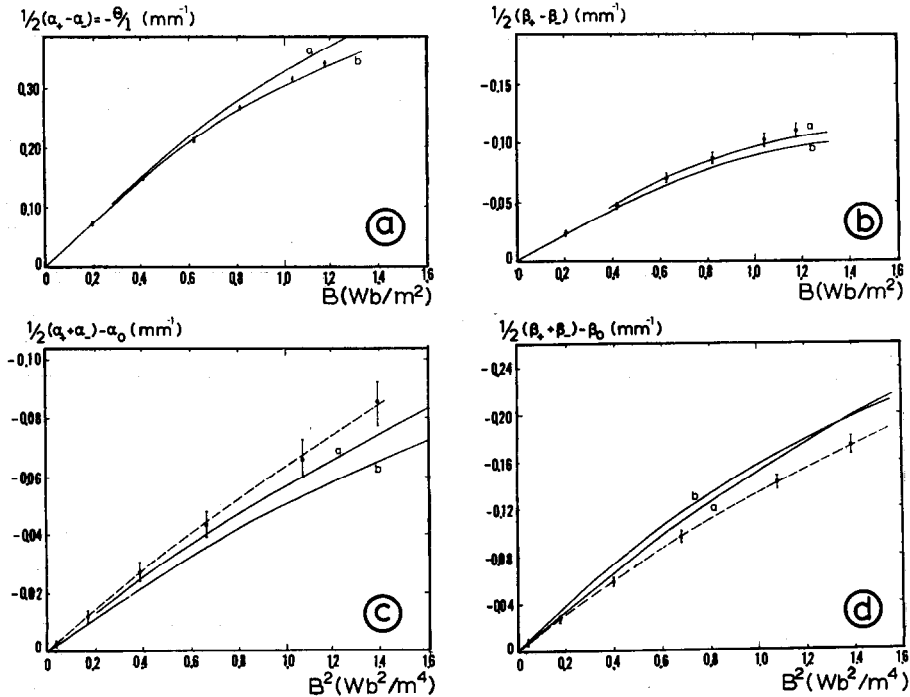


Fig. 1. Specific values of the Faraday rotation and ellipticity plotted against B (graph a, b), and of the magneto-absorption plotted against B^2 (graph c, d). *n*-type germanium, $\sigma = 24.7 \Omega^{-1}m^{-1}$, $\mu_H = 0.41 m^2/V.s$, $B \parallel [001]$, 23°C, 24.9 GHz. The points give the experimental values. The results of theoretical calculations are given by the curves, the curves (a) were calculated assuming a constant relaxation time, for curves (b) an energy dependence $\tau \propto E_n^{-\frac{1}{2}}$ was assumed.

normal theoretical picture was found. In the Voigt measurements the microwave field configuration is better understood.

Other possible sources of the deviation may be incorrect assumptions on 1) the effective mass value or 2) the scattering mechanism. The case 1) is highly improbable, the deviations are much too large to be explained with reasonable changes in the effective mass value between 4°K and 300°K^{14) 15)}. As for case 2) it may be possible that mixed scattering by both acoustical phonons ($\tau \propto E_n^{-\frac{1}{2}}$) and ionized impurities ($\tau \propto E_n^{\frac{1}{2}}$) takes place. It has been shown by Johnson and Whitesell¹⁶⁾, Jones¹⁷⁾ and recently by Krag and Brown⁸⁾ that then the Hall scattering factor can be reduced from the value 1.17 for pure acoustical phonon scattering to a value much closer to 1.0. So, in that case a description of the Hall effect with a constant relaxation time should give good results too. A computer calculation, analogous to the one performed for d.c. galvanomagnetic effects by Krag and Brown⁸⁾ would be necessary to reveal the influence of mixed scattering on the

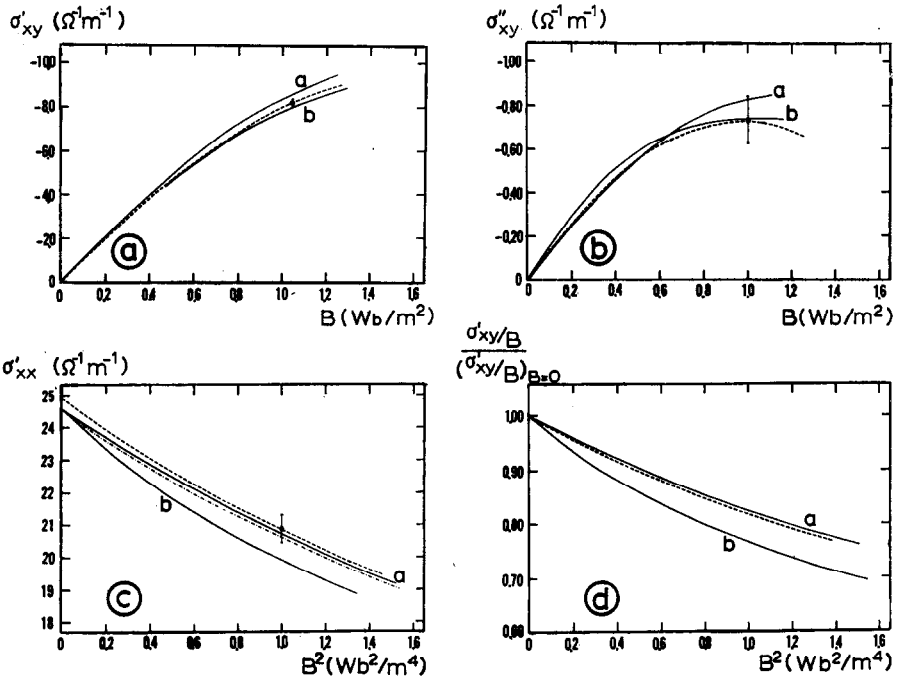


Fig. 2. Conductivity tensor elements determined with Faraday effect experiments. The dotted curves were deduced from the experimental values given in fig. 1-a-d. The solid curves were calculated with the assumption of a constant relaxation time – curves (a) – or of a relaxation time $\tau \propto E_n^{-1/2}$, curves (b). The graphs c) and d) indicate the diagonal and off-diagonal magnetoconductivity, plotted against B^2 .

Faraday effect. Such a calculation may be of value if somewhat more accurate results are available. New experiments, with a new wave guide coupler device⁹), are in progress.

The conductivity tensor elements were determined, with equations (12), from the complete Faraday effect, as given in fig. 1. In fig. 2-a, b, c the results are shown for the real part of the diagonal element, σ'_{xx} , and for the real and imaginary parts of the off-diagonal element, σ'_{xy} and σ''_{xy} . The errors indicated in the graphs correspond to the errors in fig. 1. The tensor element part σ''_{xx} is not given in fig. 2, its relative errors were rather large. The quantity σ'_{xx} is plotted against B^2 , thus giving an indication of the diagonal magnetoconductivity. In fig. 2-d the quantity σ'_{xy}/B is plotted against B^2 , this graph thus indicates the off-diagonal magnetoconductivity.

The theoretical calculations in fig. 2 are of course the same as those used for fig. 1, curves (a) again correspond to the assumption of an energy independent relaxation time, curves (b) to a relaxation time $\tau \propto E_n^{-1/2}$. It is seen that the agreement between theory and experiment is good. As for the interesting quantity σ''_{xy} , which indicates the relaxation of the electrons, this

agreement is partly accidental. The relative error is large, as a consequence of the small value of $\omega\tau$ in these experiments ($\omega\tau \simeq 0.06$).

From equation (15) it can be deduced that:

$$\frac{\sigma'_{xy}}{\sigma'_{xy}} = 2\omega\langle\tau\rangle \left[\left\langle \frac{\tau^3}{(1 + \omega^2\tau^2)^2} \right\rangle \left/ \left\langle \frac{\tau^2(1 - \omega^2\tau^2)}{(1 + \omega^2\tau^2)^2} \right\rangle \right] \langle\tau\rangle \quad (18)$$

if we assume $(\mu B)^2 \ll 1$, and anisotropic relaxation time. The latter assumption is reasonable at 300°K¹⁸). For the Hall mobility we have the relation:

$$\mu_H = \frac{K + 2}{2K + 1} \cdot \frac{e\langle\tau\rangle}{m_{\perp}} \cdot \frac{\langle\tau^2\rangle}{\langle\tau\rangle^2}, \quad K = m_{//}/m_{\perp} \quad (19)$$

Consequently, if we know the effective mass and its anisotropy we can determine a scattering factor. Inversely, if we assume a scattering law, and we know the value of K , an effective mass value can be found. From our experiments we find, for the scattering laws $\tau = \tau_0$ and $\tau \propto E_n^{-\frac{1}{2}}$, and assuming $K = 19.3$,

$$\begin{aligned} m_{\perp}/m_0 &= 0.075 \pm 15\% & (\tau = \tau_0) \\ m_{\perp}/m_0 &= 0.093 \pm 15\% & (\tau \propto E_n^{-\frac{1}{2}}) \end{aligned}$$

The value found from cyclotron resonance experiments, made at 4°K, is $m_{\perp}/m_0 = 0.082$ ¹¹). This agrees within the experimental error with our experiments, for both assumptions regarding the relaxation time.

Next, we consider the quantity $\sigma'_{xy}/B = \zeta$. The values in fig. 2-d were determined from calculations and observations between $B = 0.15$ and 1.2 Wb/m². The thus obtained curves were extrapolated to $B = 0$, and next normalized. This extrapolation introduces some uncertainty in the curves, especially in the experimental one. If we assume an isotropic relaxation time, and expand $\zeta(B)$ in powers of B^2 , retaining only the first terms of the expansion, we find from equation (15) for $\omega\tau \ll 1$:

$$\frac{\zeta(0) - \zeta(B^2)}{\zeta(0)} \simeq \mu_H^2 B^2 \frac{(2K + 1)^2}{3K(K + 2)} \cdot S, \quad S = \frac{\langle\tau^4\rangle\langle\tau\rangle^2}{\langle\tau^2\rangle^3} \quad (20)$$

An equation similar to (20) has recently been given by Furdyna¹⁹). The tangent on the $\zeta(B^2)$ curve at $B^2 = 0$, $M_{xy}(001)$, is given by:

$$M_{xy}(001) \simeq \mu_H^2 \frac{(2K + 1)^2}{3K(K + 2)} \cdot S \quad (21)$$

Consequently, it may be possible to calculate S from experimentally known values of M_{xy} , μ_H and K .

We determined S from the *calculated* curves in fig. 2-d. These calculations did not involve any expansion, as integrals in closed form were used.

Results are:

$$\begin{array}{lll} S \simeq 1.0 & (\tau = \tau_0), & \text{expected 1.00} \\ S \simeq 1.6 & (\tau \propto E_n^{-\frac{1}{2}}), & \text{expected 2.57} \end{array}$$

So, the agreement between expectations and results is rather bad. The reason may be that the equation used for M_{xy} is only valid in that range of B -values where the averaging integral (17) over the sum of the expansion terms can be replaced by the sum over the integrals. This range is restricted by the fact that the terms $\langle \tau^5 \rangle$ and higher are infinite for $\tau \propto E_n^{-\frac{1}{2}}$. Thus a separation of the B^2 terms from higher order terms is often impossible. It is reasonable that the consideration of only lower order terms of an expansion will give good results in lower order effects, for example in the conductivity ($\propto \langle \tau \rangle$), the Hall effect ($\propto \langle \tau^2 \rangle$), or even the d.c. magnetoconductivity ($\propto \langle \tau^3 \rangle$). That the expansion technique breaks down for higher order effects is not surprising.

It may be remarked that the above expansion technique can be used for σ'_{xx} too. In that case we found the same inadequacy of the expansion technique. In this connection one may note the bending of the curve (b) in fig. 2c for rather low B values.

With the foregoing considerations in mind we did not think it attractive to deduce S values from experiments.

It may be remarked that earlier Donovan and Webster⁶⁾ encountered difficulties with an expansion in which only the lower order terms were used. They noticed the inadequacy of the method in their work on the anisotropy of the Faraday effect.

5. *Anisotropy of the Faraday effect.* Finally we consider the polarization anisotropy of the Faraday effect, observed with \mathbf{B} parallel to the [011] direction of a germanium crystal. The effect can be treated formally with equations (2)-(6) and (14). We remark that, if the specific rotation is anisotropic with respect to the polarization direction of the incident wave, the observed rotation θ divided by the thickness d of the crystal will not give a specific value, but a mean value, as the polarization direction of the wave changes continuously in the propagation direction. If ϕ is the angle of the polarization direction of the incident wave with the [100] direction in the crystal, θ the observed Faraday rotation in the crystal, and $\varphi = \phi + \frac{1}{2}\theta$, then θ/d (φ) is a first approximation of the specific rotation $d\theta/dl$ (φ). With this approximate value one can calculate the corrections which are necessary because of the finite thickness of the crystal. It should be noted that the influence of boundary reflections puts a lower limit on the experimental magnitude of θ , for the value of d has to exceed the penetration depth of the microwave field at least twice⁴⁾.

In fig. 3 the results are given of measurements on the polarization aniso-

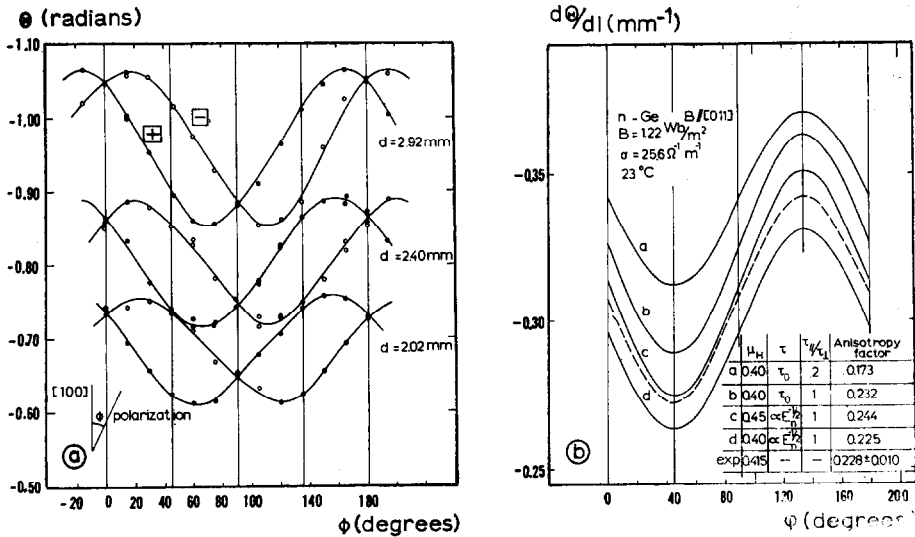


Fig. 3. a) Anisotropy of the Faraday rotation. *n*-type germanium, $\sigma \approx 25 \Omega^{-1}\text{m}^{-1}$, $\mathbf{B} // [011]$, $B = 1.22 \text{ Wb/m}^2$, 23°C , 24.9 GHz . The experimentally observed rotation θ is plotted against ϕ for three thicknesses of the crystal and for positive and negative magnetic field. ϕ is the angle between the $[100]$ orientation and the polarization of the incident microwave electric field.

b) The specific Faraday rotation $d\theta/dl$, deduced from the curves of a), plotted against the angle ϕ between the $[100]$ direction and the direction of polarization. The curves (a), (b), (c) and (d) were theoretically calculated, making different assumptions regarding the relaxation time. These assumptions are tabulated in the figure. The definition of the anisotropy factor is given in the text.

trophy of *n*-type germanium, $\sigma \approx 25 \Omega^{-1}\text{m}^{-1}$, $\mathbf{B} // [011]$, $B = 1.22 \text{ Wb/m}^2$, at 23°C . In fig. 3-a the measured rotation θ is given for positive and negative magnetic field and for three thicknesses of the crystal, as a function of the angle ϕ . The gradual shift of the maximum and minimum values from their specific positions (45° and 135°) is clearly visible.

It proved to be possible to obtain the specific rotation as a function of ϕ , by applying small corrections on $\theta/d(\phi)$ for boundary reflections and for the influence of the finite size of the crystals. The mean value of $\theta(\phi, B)$ and $\theta(180^\circ - \phi, -B)$ was used as the experimental $\theta(\phi)$ value. The result is given by the dotted curve in fig. 3-b.

Moreover, the specific polarization anisotropy was calculated, using the formalism given by Donovan and Webster⁵). The numerical values used were again $m_{||}/m_0 = 1.58$, $m_{||}/m_{\perp} = 19.3$, $\epsilon_1/\epsilon_0 = 16.3$. The measured d.c. conductivity was $\sigma = 25.6 \Omega^{-1}\text{m}^{-1}$. Two assumptions regarding the Hall mobility were made in the calculations: $\mu_H = 0.40$ and $\mu_H = 0.45 \text{ m}^2/\text{V.s}$. The different assumptions regarding the relaxation time, its energy dependence and its anisotropy, are given in the graph. The measured Hall

mobility was $\mu_H = 0.41 \text{ m}^2/\text{V.s.}$ From fig. 1-a we could conclude that for the rotation the agreement between theory and experiment was good if we assumed $\tau \propto E_n^{-\frac{1}{2}}$. So, we expect the experimental curve in fig. 3-b somewhere between the theoretical curves (c) and (d). This expectation is confirmed by experiment.

It is of interest to consider the anisotropy factor, defined as:

$$f = (\theta_{\max} - \theta_{\min}) / \frac{1}{2}(\theta_{\max} + \theta_{\min}) \quad (22)$$

This anisotropy factor of the curves $d\theta/dl(\varphi)$ was determined. Its values are given in fig. 3-b. It is seen that the agreement between experiment and theory is quite satisfactory. By a suitable interpolation between cases (c) and (d) we found:

$$\begin{aligned} f &= 0.228 \pm 0.10 && \text{(experimental)} \\ f &= 0.231 && \text{(calculated, assuming } \tau \propto E_n^{-\frac{1}{2}}, m_{//}/m_{\perp} = 19.3, \\ &&& \tau_{//}/\tau_{\perp} = 1, \mu_H = 0.41 \text{ m}^2/\text{V.s.)} \end{aligned}$$

The error in the experimental value is representative for an experimental error of about 1% in θ , this error causes a relatively large error in $(\theta_{\max} - \theta_{\min})$, and thus in the value of f .

From the anisotropy factors of the theoretical curves (a) and (b) of fig. 3 we can get an indication of the influence of the anisotropy of the relaxation time on these factors. Using this indication we obtain from the experimental results the value, assuming $m_{//}/m_{\perp} = 19.3$:

$$\tau_{//}/\tau_{\perp} = 1.03 \pm 0.10 \quad (300^\circ\text{K, } n\text{-Ge, } \sigma \simeq 25 \Omega^{-1}\text{m}^{-1}),$$

in good agreement with other workers¹⁸).

From the experimental data also the anisotropy of the ellipticity and the magneto-absorption could be deduced. The results are shown in fig. 4, for the crystal thickness $d = 2.40 \text{ mm}$. The solid curves indicate the observed experimental values of θ and Δ , and of the phase change, $\psi(B) - \psi(0)$, and the natural logarithm of the amplitude ratio, $\chi(B) - \chi(0)$, of the major axis of the ellipse, all plotted against $\varphi = \phi + \frac{1}{2}\theta$. No corrections were applied for boundary reflections. Results of calculations of the intrinsic values of θ and Δ , thus without taking into account the boundaries, are given by the dotted curves. In these calculations we assumed $\mu_H = 0.40 \text{ m}^2/\text{V.s.}$, $d = 2.50 \text{ mm}$ and τ constant. Also calculations for the value $d = 0.1 \text{ mm}$ were made.

It is seen that for θ and $\chi(B) - \chi(0)$ the maximum and minimum values appear at highly symmetrical crystal orientations ($\varphi = 45^\circ, 135^\circ$ and $0^\circ, 90^\circ$ respectively). As for the ellipticity and the phase angle of the major ellipse axis the matter is more complicated. From the calculations it followed that the extreme specific values $d\Delta/dl$ appeared at $\varphi = 45^\circ, 135^\circ$, but for larger thicknesses the extreme values were shifted. This behaviour is also shown

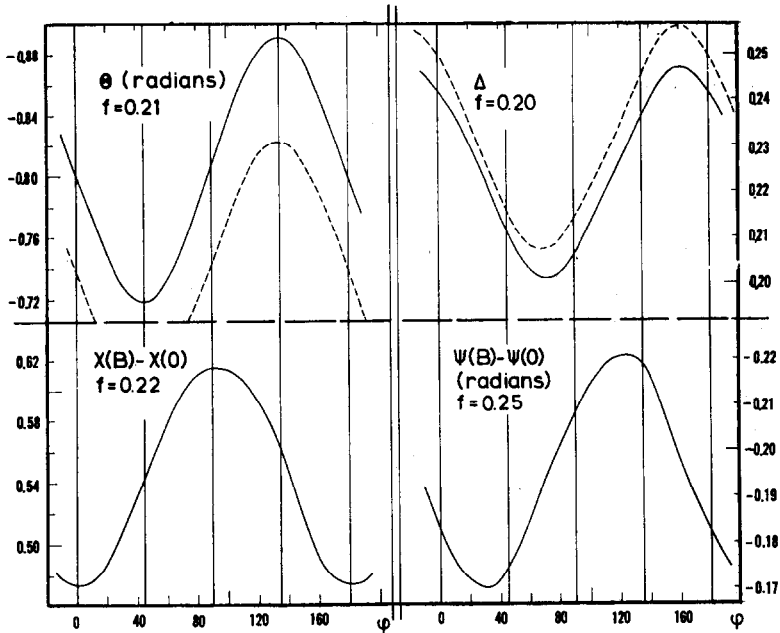


Fig. 4. Rotation, ellipticity and phase and amplitude change of the major axis of the ellipse as a function of the angle $\varphi = \phi + \frac{1}{2}\theta$, for the same crystal as in fig. 3, for 2.40 mm thickness d . Dotted curves: calculated intrinsic rotation and ellipticity, assuming $\mu_H = 0.40 \text{ m}^2/\text{V}\cdot\text{s}$ and $d = 2.50 \text{ mm}$, and $\tau \propto E_n^{-1/2}$.

by experiment. Theory and experiment are in reasonable agreement, the differences have the same sign and order of magnitude as the boundary reflection effects^{4) 9)} observed in the experiments on isotropic material (fig. 1). It should be noted that in the calculation μ_H was chosen too low and d too high.

The shift of the extreme values of Δ and $\chi(B) - \chi(0)$ makes it difficult to apply corrections for boundary reflection effects. For θ and $\chi(B) - \chi(0)$ these corrections may be applied analogous to the isotropic case, by measuring $\theta(\varphi)$ etc. as a function of the thickness of the crystal.

It is of interest to consider the factor f , as defined in (22), of all the observed quantities. It has been shown elsewhere⁹⁾ that for room temperature experiments, in which the anisotropy is not very high and the relaxation small, one might expect that these factors f are almost equal for the rotation and the ellipticity. This is confirmed by experiment, compare fig. 4. Moreover, it seems that the same factor f appears in the anisotropy of the magneto-absorption. This implies that only one information can be obtained from the two measurements of the anisotropy factors of θ and Δ . This fact, added to the circumstance that it is difficult to deduce the anisotropy of the specific ellipticity from experiments, makes a measurement a little unattractive.

6. *Conclusions.* From the experiments, described in the foregoing, we may draw the following conclusions:

a) It was possible to deduce the conductivity tensor elements from the complete Faraday effect, measured with the wave guide coupler device. The agreement between theory and experiment, both for the complete Faraday effect and the conductivity tensor elements, was fairly satisfactory. Assuming a scattering law for the current carriers it was possible to obtain a value of the effective mass at 300°K from the complex off-diagonal tensor element. The mass value found agreed within the experimental error with the cyclotron resonance mass value (4°K). However, our experiments were not accurate enough for a reliable study of scattering mechanisms at room temperature. Moreover, it turned out that the higher order scattering factors, appearing in an expansion of the Faraday effect in a series in B^2 , cannot give information about the scattering mechanism.

b) The polarization anisotropy of the Faraday effect could be determined with a fair accuracy. From the anisotropy of the rotation a value of the relaxation time anisotropy could be deduced. It seemed that, at least in room temperature experiments, the same information could be obtained from measurements of the anisotropy of the rotation and of the ellipticity. Moreover, the interpretation of the ellipticity measurements is hampered by the unknown influence of boundary reflections on the results obtained. In our case this influence could not be eliminated in a simple way.

Acknowledgement. This investigation is part of the research program of the "Stichting voor Fundamenteel Onderzoek der Materie", and was made possible by financial support from the "Nederlandse Organisatie voor Zuiver Wetenschappelijk Onderzoek".

Received 20-7-65

REFERENCES

- 1) Rau, R. and Caspari, M. E., Phys. Rev. **100** (1955) 632.
- 2) Furdyna, J. K. and Broersma, S., Phys. Rev. **120** (1960) 1995.
- 3) Furdyna, J. K. and Brodwin, M. E., Phys. Rev. **132** (1963) 97.
- 4) Bouwknecht, A. and Volger, J., Physica **30** (1964) 113.
- 5) Donovan, B. and Webster, J., Proc. Phys. Soc. **79** (1962) 46, 1081.
- 6) Donovan, B. and Webster, J., Proc. Phys. Soc. **81** (1963) 90.
- 7) Champlin, K. S., Physica **28** (1962) 1143.
- 8) Krag, W. E. and Brown, M. C., Phys. Rev. **134** (1964) A 779.
- 9) Bouwknecht, A., Thesis, University of Utrecht (1965).
- 10) Dingle, R. B., Arndt, D. and Roy, S. K., Appl. sci. Res. **B 6** (1957) 144.
- 11) Levinger, B. W. and Frankl, D. R., J. Phys. Chem. Solids **20** (1961) 281.
- 12) Baynham, A. C., Gibson, A. F. and Granville, J. W., Proc. Phys. Soc. **75** (1960) 306.

- 13) Bouwknecht, A. and Volger, J., Proc. Int. Conf. Phys. Semiconductors Paris (1964) 281. (Dunod, Paris 1964).
- 14) Cardona, M., Paul, W. and Brooks, H., Helv. phys. Acta **33** (1960) 329.
- 15) Ukhanov, Y. I. and Maltsev, Y. V., Soviet Phys. Solid State **5** (1964) 2144.
- 16) Johnson, V. A. and Whitesell, W. J., Phys. Rev. **89** (1953) 941.
- 17) Jones, H., Phys. Rev. **81** (1951) 149.
- 18) Paige, E. G. S., Progress in Semiconductors 8. (Heywood. London, 1964).
- 19) Furdyna, J. K., Phys. Rev. Letters **13** (1964) 426.